HHS Public Access

Author manuscript

Biomacromolecules. Author manuscript; available in PMC 2024 February 13.

Published in final edited form as:

Biomacromolecules. 2023 February 13; 24(2): 849–857. doi:10.1021/acs.biomac.2c01269.

Targeted Drug Delivery Using a Plug-to-Direct Antibody-Nanogel-Conjugate (ANC)

Uyen Huynh[a,‡], **Peidong Wu**[a,‡], **Jingyi Qiu**[b], **Theeraphop Prachyathipsakul**[a], **Khushboo Singh**[a], **D. Joseph Jerry**[c,d,*], **Jingjing Gao**[a,*], **S. Thayumanavan**[a,b,c,*]

[a]Department of Chemistry, University of Massachusetts, Amherst, Massachusetts 01003, United States.

[b]Department of Biomedical Engineering, University of Massachusetts, Amherst, Massachusetts 01003, United States.

[c]Center for Bioactive Delivery, Institute for Applied Life Sciences, University of Massachusetts, Amherst, Massachusetts 01003, United States.

[d]Department of Veterinary and Animal Sciences, University of Massachusetts, Amherst, Massachusetts 01003, United States.

Abstract

Targeted drug delivery using antibody-drug conjugates (ADCs) have attracted great attention due to the enhanced therapeutic efficacy compared to traditional chemotherapy. However, the development has been limited due to low drug-to-antibody ratio and laborious linker-payload optimization. Herein, we present a simple and efficient strategy to combine favorable features of polymeric nanocarriers with antibodies to generate an antibody-nanogel conjugate (ANC) platform for targeted delivery of cytotoxic agents. Our nanogels stably encapsulate several chemotherapeutic agents ranging in mechanism of actions and solubility. We showcase the targetability of ANCs and their selective killing of cancer cells over-expressing disease relevant antigens such as HER2, EGFR, and tMuc1, which cover a broad range of breast cancer cell types, while maintaining low to no toxicity to non-targeted cells. Overall, our system represents a versatile approach that could impact next generation nanomedicine in antibody-targeted therapeutics.

Graphical Abstract

[*]Corresponding Author: S. Thayumanavan - Department of Chemistry, Department of Biomedical Engineering, and Center for Bioactive Delivery, Institute for Applied Life Sciences, University of Massachusetts, Amherst, Massachusetts 01003, United States; thai@umass.edu.; Jingjing Gao - Department of Chemistry, University of Massachusetts, Amherst, Massachusetts 01003, United States. jgao16@bwh.harvard.edu; D. Joseph Jerry - Department of Veterinary and Animal Sciences, University of Massachusetts, Amherst, Massachusetts 01003, United States. jjerry@vasci.umass.edu.

[‡]These authors contributed equally.

Author Contributions

The manuscript was written through contributions of all authors. All authors have given approval to the final version of the manuscript.

Supporting Information. The following files are available free of charge at pub.acs.org.

Materials and experimental methods; polymer synthesis and characterizations; additional in vitro characterizations using flow cytometry and confocal microscopy; cytotoxicity results of free drugs (PDF)

The authors declare no conflict of interest.

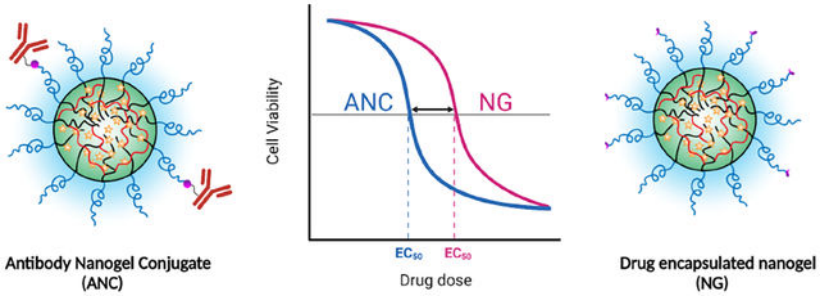

Keywords

Targeted delivery; antibody nanogel conjugate; drug encapsulation; intracellular drug delivery; antibody conjugation

INTRODUCTION

Targeted drug delivery using antibody-drug conjugates (ADCs) offers the means to specifically kill cancer cells where the damage to other tissues is greatly reduced compared to traditional chemotherapy.[1–5] The ADC approach couples the specificity of monoclonal antibodies with the cytotoxicity of chemotherapeutic drugs, which is leading the new era of targeted cancer therapy with fourteen approved ADCs and more than 100 ADC candidates under clinical evaluation to date.[6–9] For example, trastuzumab (Herceptin) antibody has been exploited for its specificity to bind to human epidermal growth factor receptor 2 (HER2) to generate the ADC, Kadcyla (trastuzumab-SMCC-DM1), by conjugating it with the drug emtansine (DM1). This ADC formulation has significantly improved the invasive disease-free survival of HER2-positive breast cancer patients by 50%, compared to trastuzumab alone.[10,11] While Kadcyla has been only used for HER2+ breast cancer,[12,13] recent approval of sacituzumab govitecan, based on an anti-trophoblast cell-surface antigen 2 (Trop-2) ADC, has broadened the scope of ADCs for pretreated metastatic triple-negative breast cancer (TNBC).[14,15] Despite these successes, the clinical potential of ADCs has not been fully realized because: (i) the low drug-to-antibody ratio (DAR) in the current ADC format requires the use of highly toxic drugs, making off-target toxicity a significant limitation; and (ii) the antibody-drug linker stability and degradability requirements make their design laborious and limits the drugs that are amenable to be an ADC component.[1,16,17] Efforts to overcome such drawbacks includes utilizing peptide, aptamer or folate receptor as the targeting moieties.[18] Specifically, folate receptors a (FRa) is unique in its high expression in tumor cells. A folate-maytasinoid conjugate had been shown to show high efficacy in oral squamous carcinomas.[19] Similarly, peptide and aptamer-drug conjugates with easy synthesis and higher tumor penetration have also attracted interest in targeted therapies. In contrast to ADCs, these conjugates are easier to manufacture, they offer well-defined structures, higher drug loading, good stability, and better tumor penetration. However, they are typically associated with faster clearance and have abridged affinity and specificity to cancer cells.[20,21] Next generation targeted nanomedicine highlighted the importance of polymer-drug conjugates which can minimize these limitations. Depending on the nature of the polymer and drug content, polymer-drug conjugates might form different

nanostructures such as micelles, nanogels or nanocomplexes. All offer high stability, high drug loading and ease of synthesis. Furthermore, conjugation with antibody offers great affinity towards specific cancer cells and enhanced pharmacokinetics of the system. A few antibody-nanogel/polymersome conjugates have been developed and showed efficacy in many tumor models including multiple myeloma, glioma, triple-negative breast cancer and pancreatic cancer.[22–25] Herein, we present a simple and efficient antibody-nanogel conjugate (ANC) platform that overcomes these shortcomings by combining the favorable features of polymeric nanocarriers with antibodies.[26–29]

The ANCs are based on polymeric nanogels that stably and non-covalently encapsulate many chemotherapeutic agents ranging in the mechanism of actions and solubility. Here, the targeting antibodies are conjugated to the surface of the nanogel through the polymer chain. This latter feature, combined with the non-covalent drug encapsulation mode, obviates the complex linker requirements, and consequently, expands the scope of drugs that can be used in this format. Similarly, while the DAR of ADCs are typically between 4 and 8, the DAR of ANCs can conveniently be 10^2–10^6 times higher, depending on the size of the nanogel and the drug loading capacity.[30–32] Overall, our ANC system is a versatile nanocarrier platform that features: (i) easily functionalized surface for antibody decoration, (ii) simple preparation protocols; (iii) high drug loading capacity for a broad range of drugs; (iv) low vehicle toxicity; and (v) triggerable on-demand release of cargo at targeted sites. In this report, we demonstrate the versatility of the ANC platform with three disease-relevant antibodies and four chemotherapeutic drugs, highlighting the broad applicability of the ANCs in cancer therapy.

MATERIALS AND METHODS

Materials.

PEG_{5000} RAFT, NHS RAFT, methacryloyl chloride, AIBN, and DiI were purchased from Sigma-Aldrich. Boc-NH-PEG_{5000}-NH_2 was purchased from Laysan Bio. DBCO-PEG_5-NHS ester was purchased from BroadPharm. trifluoroacetic acid (TFA), triethylamine (TEA) were purchased through Fisher Scientific. Trastuzumab was purchased from Selleck Chemicals. TAB 004 anti-tMuc1 antibody was purchased from Creative Biolab. Anti-EGFR antibody was purchased from BioXCell. All the drugs were purchased from MedChemExpress. All molecules without characterization data mentioned below were synthesized through well-established synthesis procedures previously reported by our group and are appropriately referenced.

Polymer synthesis.

PEG-PDS block copolymer (PEG-PDS-BCP) was synthesized by a reversible addition fragmentation chain transfer (RAFT) polymerization of either methoxy terminated or Boc terminated PEG5000RAFT monomer and pyridyl disulfide ethyl methacrylate (PDSMA). The Boc terminated polymer was then deprotected and the amine functional group was reacted with an N3-PEG3-NHS linker to yield the azide terminated PEG-PDS-BCP. After purification of the polymer, the monomer composition was calculated to contain

10 repeating unit of PDS per PEG block. Detailed procedures for the preparation of the methoxy and azide terminated polymers are available in Supporting Information.

Nanogel preparations.

Methoxy terminated PEG-PDS-BCP (P1) and azide terminated PEG-PDS-BCP (P4) were freshly prepared at 50 mg/mL in DMSO. All the drugs and DiI were freshly prepared at a concentration of 10 mg/mL in DMSO. 20 μL of P1 and 20 μL of P4 were mixed with a 30 μL (15 wt%) drug or 20 μL (10 wt%) DiI stock solution. To this mixture of polymer and drugs or DiI, 1 mL of HPLC grade water was added with immediate sonication in a sonication bath for 5–10 mins until the nanogel solution is clear. DMSO was purified by dialysis against DI water using a mini dialysis kit (1 kDa cutoff) from Cytiva for 6 hrs. After that, the nanogels were crosslinked using 7.7 μL of DTT (stock solution in water, 5 mg/mL) to target a 20% crosslinking density. After 3 hrs of crosslinking, nanogels were dialyzed against water for 24hrs using a mini dialysis kit (8 kDa cutoff) to remove byproducts and unencapsulated drugs. The final polymer concentration of nanogels was calibrated to 2 mg/mL.

Antibody Modification.

Antibodies were buffer exchanged into a conjugation buffer (PBS pH 7.5, 50 mM K_2HPO_4, 100 mM NaCl) and concentrated to > 5 mg/mL using Amicon ultra centrifugal kit (30 kDa cutoff). The concentration of antibodies was calibrated using UV absorbance at 280 nm. DBCO-PEG_5-NHS ester was freshly prepared in DMSO at a concentration of 10 mM. To a solution of 20 μL antibody at 5 mg/mL (100 μg) in the conjugation buffer, 1 μL of 10 mM DBCO-PEG_5-NHS ester linker in DMSO (15 eq) was added. The mixture was incubated at 4 °C for 16 hrs. The excess DBCO linker was purified by Amicon ultra centrifugal kit (30 kDa cutoff) for 6 times. The final concentration of antibodies was calibrated by Nanodrop.

Antibody nanogel conjugation.

The antibody nanogel conjugation was carried out by incubating a mixture of 300 μL nanogel solution (0.6 mg polymer) and 0.2 mg DBCO modified antibody for 48 hrs at 4 °C. Free antibodies were purified by dialysis against deionized water for 48 hrs at 4 °C using a 300 kDa Float-A-Lyzer™ from Spectrum™. The final concentration of drug and dye was calibrated by HPLC or UV. Antibody concentration was calculated using Pierce™ BCA Protein Assay from ThermoFisher. Detailed drug and antibody quantification procedures are available in Supporting Information.

Cell culture.

Tumor cell lines (Breast carcinoma SKBR3, BT474, MD-MB-468, ovarian carcinoma SKOV3) and normal breast epithelial cells MCF10A were purchased from the American Type Culture Collection (ATCC). BT474 and MDA-MB-468 were maintained in Ham's F-12: high glucose DMEM (50:50) supplemented with 10% FBS, 100 units/mL of penicillin, and grown in 5% CO_2 incubator. SKBR3 cells were grown in McCoy's 5A media supplemented with 10% FBS, 100 units/mL of penicillin, and grown in 5% CO_2 incubator. MCF10A cells were grown in DMEM:F12 media (Gibco, Fisher cat. No.: 11-320- 082)

supplemented with 1% 1M HEPES, 1% of L-glutamine (Gibco, Fisher cat. No.: 25-030-081), 750 uL of 10 mg/mL gentamicin (Fisher BioReagents; Fisher cat. No. BP918–1), 5% FBS, 500uL of 10 mg/mL insulin, 1 mL of 10 μg/mL EGF (human), 100 uL of 500 μg/mL cholera enterotoxin and 5mL of 50 μg/mL hydrocortisone grown in 5% CO_2 incubator.

Flow cytometry.

0.4 million of SKOV3, SKBR3, and MCF10A cells were treated with DiI encapsulated nanogel, with and without anti-HER2 conjugations, namely anti-HER2-ANC and NG, respectively. The amount of anti-HER2-ANC and NG were added according to the DiI concentration, which was calibrated using UV-vis. Cells were incubated at different time points (10 mins, 30 mins and 1h). Then, the media was removed, and cells were washed twice with PBS. Cells were then trypsinized, quenched with media, transferred to centrifuge tubes and spun at 2000 rpm for 5 minutes. Subsequent washing and analysis with flow cytometry were performed similarly as described in the receptor expression section (Supporting Information). All studies were performed in triplicate.

Confocal Imaging.

1×10^4 cells were first plated onto a 4-chamber, 35 mm glass-bottom dishes and incubated at 37 °C in 5% CO_2 overnight. Then, cells were washed once with PBS before treated with new media containing 30 μg/mL DiI-NC or anti-HER2-DiI-ANC at the same DiI concentration (normalized by UV-vis). After incubating at 37 °C for 30 mins (10 mins for anti-EGFR-DiI-ANC and DiI-NG), cells were washed twice with PBS and fresh media were added and continued incubating for 4 h. To prepare for visualization, the cells were washed with PBS and then stained with Hoechst 33342 (Invitrogen). Assessment of ANC and NG intracellular uptake was recorded using a 560 nm laser, and the nuclear stain was detected using a 405 nm wavelength laser. Imaging was performed on a Nikon Ti2 stand with a spinning disk confocal and 2 camera TIRF system. Co-localization of blue (Hoechst) and red (Cy5) channels were studied to evaluate the location of the dye-encapsulated particles.

Cell viability assay.

Cells were seeded on opaque flat-bottom 384-well tissue culture plates at a density of 1250 cells/well and rested for 24 h at 37 °C in 5% CO_2. After incubation, the culture medium was removed, and cells were treated with fresh media containing ANC and NG samples at different concentrations for 10 mins. Then, media was removed, cells were washed twice with PBS, and fresh media was added and incubated for 48h. After treatments, cells were treated with Cell Titer-Glo reagent for 10 min at room temperature and the luminescent signal was measured using a SpectraMax iD5 multi-mode microplate reader.

RESULTS AND DISCUSSION

Nanogels were prepared by the assembly of amphiphilic block copolymers that were synthesized through RAFT polymerization, which contains polyethylene glycol (MW 5000) as the hydrophilic block and pyridyl disulfide (PDS) ethyl methacrylate as the hydrophobic block (Scheme 1). Crosslinked nanogels fabricated from PEG-PDS block copolymers exhibit high drug loading capacity, stable encapsulation, and tunable release kinetics

compared to our previously reported random copolymers.[32,33] To provide an accessible handle for antibody conjugation, we synthesized these polymers with an azide functional group at the terminus of the hydrophilic PEG chain (Scheme S1). By co-assembling the azide terminated polymer and the corresponding methoxy-terminated polymer[31,34], we prepared nanogels with controlled presentation of azide functionality handles on their surface. This offers a simple and efficient approach for post-assembly modification of the nanogels with targeting antibodies *via* the efficient strain-promoted alkyneazide cycloadditions (SPAAC).[35,36] For the initial proof-of-concept, we chose trastuzumab as the antibody to generate anti-HER2-ANC. The antibody was first modified with a DBCO-PEG5-NHS ester linker, followed by conjugation with azide functionalized nanogel at pH 7.4 (Scheme 1). The resultant anti-HER2-ANC was purified by dialysis. The size of the anti-HER2-ANC is ~100 nm, as measured by both dynamic light scattering (DLS) and transmission electron microscopy (TEM) (Figure S10).

Next, we are interested in evaluating the targeting capability of anti-HER2-ANC in cancer cell lines expressing different levels of HER2 receptors. SKBR3 and SKOV3 are both cancer cell lines that overexpress HER2, while the normal breast cell MCF10A expresses low levels of HER2. To independently confirm the HER2 expression levels, we examined the expression levels of HER2 on the surface of these cells by flow cytometry. SKBR3 was found to express the highest levels of HER2 receptors while MCF10A has minimal expression (Figure 1a). Then to evaluate the targeting specificity of anti-HER2-ANC, we encapsulated a hydrophobic fluorophore, 1,1’-dioctadecyl-3,3,3’,3’-tetramethylindocarbocyanine perchlorate (DiI) into the anti-HER2-ANC. The uptake of ANCs into cancer cell lines expressing different levels of HER2 receptors was then monitored using flow cytometry. To evaluate the relative efficacy of targeted cellular uptake of ANCs, we optimized the incubation time. DiI-encapsulated nanogel and ANC were incubated in MCF10A and SKBR3 cells for 10 mins, 30 mins, and 1h in a flow cytometry study. First, the difference in fluorescence intensity between the nanogel and the ANC in SKBR3 cells is more significant than that in SKOV3 cells with incubation at 10 mins (Figure 1b), which is consistent with the differences in HER2 expression levels. The fluorescence difference between the nanogel and the ANC decreased with increasing incubation time (Figure S14), suggesting that the antibody-directed cell-specific recognition and uptake is very fast. Following this study, 10 mins incubation time was chosen for further experiments to better reveal the cell-specific recognition process of ANCs.

We also evaluated the cellular uptake of DiI loaded-ANC and the nanogel by confocal laser scanning microscopy (CLSM). A significant fluorescence signal was observed in SKBR3 cells treated with HER2-ANC, but a limited fluorescence signal was found with nanogel treated cells, suggesting the anti-HER2 antibody plays important role in promoting cellular uptake. Moreover, enhanced uptake was also observed in SKBR3 cells with antiHER2-ANC compared to the nanogel, but not in MCF10A cells (Figure 1c), which further indicates that the surface decorated trastuzumab aided in cell-specific recognition and uptake of nanogels in HER2-overexpressed breast cancer cell lines.

Next, we utilized the ANC platform to deliver chemotherapeutic drugs to cancer cells. Different classes of chemotherapeutic drugs can inhibit tumor growth and induce apoptosis

via various mechanisms. To accommodate a specific anticancer drug for a certain cancer type, traditional polymer-based drug delivery systems require extensive structural optimization of the backbone or the cargos for efficient encapsulation and stability. Here, we aimed to demonstrate that our nanogel system can provide a modular platform that can stably encapsulate cargos with different physiochemical properties. This versatility of the ANCs was first exemplified by non-covalent encapsulation of drugs with varied hydrophobicity, *viz.*, doxorubicin (DOX; logP: 0.57), 7-ethyl-10-hydroxy-camptothecin (SN38; logP: 2.67), and paclitaxel (PTX; logP: 4.95). Then we also successfully loaded mertansine (DM1) to the nanogel, which can covalently conjugate to the hydrophobic block of the polymer chains through thiol-disulfide exchange reaction. Encapsulation stability and tunable release properties of these nanogels have been investigated previously.[31,32] After the conjugation of antibodies to the nanogels, we observed a 5 nm increase in size for ANCs (Figure S10). The success of antibody modification was also confirmed by the change in the zeta potential of the nanogels before and after antibody conjugation. We observed an increase in zeta potential after antibody conjugation at pH 7 due to the positively charged trastuzumab[36] (Figure S10). We then evaluated the stability of these ANCs in PBS buffer 7.4 for 5 days, where negligible changes in sizes were observed in all four ANCs (Figure S11).

Then we focused on determining the DAR values for the developed ANC. Increasing the drug-to-antibody ratio (DAR) for ADC to be more than 4:1 has been a longstanding challenge, which significantly impeded the further development of ADCs.[37–40] Our ANC platform uniquely positioned us to address this challenge by increasing the DAR without compromising the stability and targeting capability of antibodies. We performed theoretical calculations of DAR values based on reasonable assumptions in the physical properties such as density and volume of our nanogel. We found that with either non-covalent or covalent encapsulation, the DAR values can range between 10^2 – 10^5 (Figure S13). This enormous tunability in DAR could expand the repertoire of drugs for cancer therapy. Here, we formulate the ANCs using 15% wt. drug feed and a 1:5 (antibody /NG wt.) antibody dosage. We then calculated the DAR of ANCs by quantifying the antibody concentration in the ANC using BCA assay and drug concentration using HPLC. The DAR values of all ANCs were calculated by the ratios of drug concentration over the antibody concentration, which are reported in Table 1. Note that we can further fine tune the DAR, if necessary, by simply varying the amount of drug feeding and degree of antibody conjugation on the nanogel surface.

We then evaluated the cytotoxicity of these ANCs towards cancer cells with varied HER2 expression levels. Higher potency of ANCs compared to NGs was observed in HER2-positive SKOV3 and SKBR3 cell lines compared to MCF10A cells (Figure 2, Table 2), suggesting the efficient uptake of anti-HER2 conjugated ANCs due to receptor-mediated uptake. DM1-ANC showed a significant increase in cytotoxicity in both SKOV3 and SKBR3 cell lines while cytotoxicity of DOX-ANC is notably higher than DOX-NG in SKOV3 cell line. However, the gain in cytotoxicity of PTX-ANC and SN38-ANC comparing to NG is less significant which is attributed to the inherently lower drug sensitivity to the cells (Figure S16). This observation highlights the importance of choosing the right cytotoxic drug cargo for the ANCs. Most importantly, ANC showed similar or less

toxicity in HER2-negative MCF10A cells which stressed the importance of the antibody-antigen recognition process that holds great potential to minimize off-target effects.

Inspired by the results from Trastuzumab-ANCs towards HER2-expressing cancer cells, we tested the applicability of ANCs to target cells with different overexpressed receptors, especially in HER2-negative breast cancer subtypes. Specifically, tumor-specific mucin 1 (tMuc1) and epidermal growth factor receptor (EGFR) show great potential in different breast cancer subtypes.[41,42] In contrast to tumor tissue where the tMuc1 epitope is exposed, the Muc1 epitope in healthy tissue is highly glycosylated masking the epitope.[43,44] The unique glycosylation status and common appearance in breast cancers (>90%) of mucin 1 proteins are quite appealing for the development of ADCs that specifically target tMuc1.[43,45,46] In this work, we conjugated anti-tMuc1 antibody, TAB004, to the nanogels to target tMuc1-positive breast cancer cells. The choice of cargo was established from an IC50 screening of four commonly used drugs including DOX, PTX, DM1, and SN38, where SN38 showed the highest sensitivity to both tMuc1 and EGFR expressing cell lines (Figure S17). We prepared anti-tMuc1-ANC that is loaded with either DiI or SN38 to check the cellular uptake and anti-cancer efficacy in both tMuc1-positive (T47D) and -negative (BT474) cell lines. The expression levels of tMuc1 receptors in both cell lines were shown in Figure 3b. A positive trend was observed where tMuc1-ANC could specifically attach to the surface of T47D cells and cause enhanced receptor-mediated cellular uptake shown in both confocal imaging (Figure 3a, Figure S15b) and flow cytometry (Figure 3c). Similarly, cytotoxicity evaluation of anti-tMuc1-SN38-ANC and SN38-nanogel showed higher toxicity in T47D cells (Figure 3e) but not in BT474 cells for the ANCs (Figure 3d). This highlighted the significance of the ANC in minimizing toxicity towards non-targeted tissues.

To further demonstrate the broader applicability of the ANC platform, we developed anti-EGFR-conjugated nanogels because EGFR is overexpressed in about half of the triple-negative breast cancer patients.[42,47] Briefly, surface receptor expression level and cellular uptake of nanogels in comparison to ANC towards MDA-MB-468 (EGFR-positive) and MCF10A (EGFR-low) cells were evaluated (Figure 4b). Here, anti-EGFR-ANC consistently showed higher specificity toward EGFR-positive cells in both flow cytometry and confocal imaging experiments (Figure 4a and 4c). The superior efficacy of ANC was also confirmed from toxicity studies where anti-EGFR-SN38-ANC acquires more than 5-fold lower IC50 values compared to the nanogel (Figure 4e). Expectedly, the toxicity of ANC is comparable to that of NG in the EGFR-low MCF10A cell line (Figure 4d).

CONCLUSIONS

In summary, we demonstrate here a polymer-based Antibody Nanogel Conjugate (ANC) platform that can successfully deliver chemotherapy drugs to specific cancer cells. This platform holds great potential as a next-generation nanomedicine for targeted delivery, because i) the polymeric nanogel itself is non-toxic and easy to prepare;[31–34] ii) this platform can accommodate a variety of chemotherapy drugs through covalent or non-covalent encapsulation; iii) by a simple “plug-and-play” strategy, various antibodies could be utilized to achieve cell-specific delivery of drugs; iv) the drug to antibody ratio of ANC can be increased by orders of magnitude; and v) the stably-encapsulated cargo can be

released by the intracellular redox environment. In addition to these exciting features, we have also developed a well-established protocol for ANC preparation and characterization to ensure stability and efficacy. Overall, the ANC platform offers a new avenue to substantially enhance the scope of antibody-based targeting of chemotherapeutic delivery to cancer cells.

Supplementary Material

Refer to Web version on PubMed Central for supplementary material.

Funding Sources

We thank partial support from the National Institute of Health (GM-136395). We also thank support from the Institute for Applied Life Sciences (IALS) of UMass Amherst.

ABBREVIATIONS

ADC	antibody drug conjugate
ANC	antibody nanogel conjugate
NG	nanogel
DAR	drug-to-antibody ration
RAFT	reversible addition fragmentation chain transfer
HER2	human epidermal growth factor receptor 2
ER	estrogen receptor
MFI	mean fluorescence intensity
DLS	dynamic light scattering
TEM	transmission electron microscope

REFERENCES

(1). Gordon MR; Canakci M; Li L; Zhuang J; Osborne B; Thayumanavan S Field Guide to Challenges and Opportunities in Antibody-Drug Conjugates for Chemists. Bioconjug. Chem 2015, 26 (11), 2198–2215. 10.1021/acs.bioconjchem.5b00399. [PubMed: 26308881]

(2). Das R; Kanjilal P; Medeiros J; Thayumanavan S What's Next after Lipid Nanoparticles? A Perspective on Enablers of Nucleic Acid Therapeutics. Bioconjug. Chem 2022, 33 (11), 1996–2007. 10.1021/acs.bioconjchem.2c00058. [PubMed: 35377622]

(3). Weiner GJ Building Better Monoclonal Antibody-Based Therapeutics. Nat. Rev. Cancer 2015, 15 (6), 361–370. 10.1038/nrc3930. [PubMed: 25998715]

(4). Buss NAPS; Henderson SJ; McFarlane M; Shenton JM; De Haan L Monoclonal Antibody Therapeutics: History and Future. Curr. Opin. Pharmacol 2012, 12 (5), 615–622. 10.1016/j.coph.2012.08.001. [PubMed: 22920732]

(5). Li J; Zhu Z Research and Development of next Generation of Antibody-Based Therapeutics. Acta Pharmacol. Sin 2010, 31 (9), 1198–1207. 10.1038/aps.2010.120. [PubMed: 20694021]

(6). Fu Z; Li S; Han S; Shi C; Zhang Y Antibody Drug Conjugate: The "Biological Missile" for Targeted Cancer Therapy. Signal Transduct. Target. Ther 2022, 7 (1), 1–25. 10.1038/s41392-022-00947-7. [PubMed: 34980881]

(7). Ross JS; Gray K; Schenkein D; Greene B; Gray GS; Shulok J; Worland PJ; Celniker A; Rolfe M Antibody-Based Therapeutics in Oncology. Expert Rev. Anticancer Ther 2003, 3 (1), 107–121. 10.1586/14737140.3.1.107. [PubMed: 12597355]

(8). Venugopal S; Daver N; Ravandi F An Update on the Clinical Evaluation of Antibody-Based Therapeutics in Acute Myeloid Leukemia. Curr. Hematol. Malig. Rep 2021, 16 (1), 89–96. 10.1007/s11899-021-00612-w. [PubMed: 33630233]

(9). Pourjafar M; Samadi P; Saidijam M MUC1 Antibody-Based Therapeutics: The Promise of Cancer Immunotherapy. Immunotherapy 2020, 12 (17), 1269–1286. 10.2217/imt-2020-0019. [PubMed: 33019839]

(10). Mamounas EP; Untch M; Mano MS; Huang CS; Geyer CE; von Minckwitz G; Wolmark N; Pivot X; Kuemmel S; DiGiovanna MP; Kaufman B; Kunz G; Conlin AK; Alcedo JC; Kuehn T; Wapnir I; Fontana A; Hackmann J; Polikoff J; Saghatchian M; Brufsky A; Yang Y; Zimovjanova M; Boulet T; Liu H; Tesarowski D; Lam LH; Song C; Smitt M; Loibl S Adjuvant T-DM1 versus Trastuzumab in Patients with Residual Invasive Disease after Neoadjuvant Therapy for HER2-Positive Breast Cancer: Subgroup Analyses from KATHERINE. Ann. Oncol 2021, 32 (8), 1005–1014. 10.1016/J.ANNONC.2021.04.011/ATTACHMENT/528B5739-F336-4769-B616-D994A6AEE803/MMC1.DOCX. [PubMed: 33932503]

(11). Wedam S; Fashoyin-Aje L; Gao X; Bloomquist E; Tang S; Sridhara R; Goldberg KB; King-Kallimanis BL; Theoret MR; Ibrahim A; Amiri-Kordestani L; Pazdur R; Beaver JA FDA Approval Summary: Ado-Trastuzumab Emtansine for the Adjuvant Treatment of HER2-Positive Early Breast Cancer. Clin. Cancer Res 2020, 26 (16), 4180–4185. 10.1158/1078-0432.CCR-19-3980. [PubMed: 32217612]

(12). Figueroa-Magalhães MC; Jelovac D; Connolly RM; Wolff AC Treatment of HER2-Positive Breast Cancer. Breast 2014, 23 (2), 128–136. 10.1016/j.breast.2013.11.011. [PubMed: 24360619]

(13). Loibl S; Gianni L HER2-Positive Breast Cancer. Lancet 2017, 389 (10087), 2415–2429. 10.1016/S0140-6736(16)32417-5. [PubMed: 27939064]

(14). Guerra E; Alberti S The Anti-Trop-2 Antibody-Drug Conjugate Sacituzumab Govitecan—Effectiveness, Pitfalls and Promises. Ann. Transl. Med 2022, 10 (9), 501–501. 10.21037/atm-22-621. [PubMed: 35928735]

(15). Goldenberg DM; Sharkey RM Sacituzumab Govitecan, a Novel, Third-Generation, Antibody-Drug Conjugate (ADC) for Cancer Therapy. Expert Opin. Biol. Ther 2020, 20 (8), 871–885. 10.1080/14712598.2020.1757067. [PubMed: 32301634]

(16). Coats S; Williams M; Kebble B; Dixit R; Tseng L; Yao NS; Tice DA; Soria JC Antibody-Drug Conjugates: Future Directions in Clinical and Translational Strategies to Improve the Therapeutic Index. Clin. Cancer Res 2019, 25 (18), 5441–5448. 10.1158/1078-0432.CCR-19-0272. [PubMed: 30979742]

(17). Beck A; Goetsch L; Dumontet C; Corvaïa N Strategies and Challenges for the next Generation of Antibody-Drug Conjugates. Nat. Rev. Drug Discov 2017, 16 (5), 315–337. 10.1038/nrd.2016.268. [PubMed: 28303026]

(18). Wang Z; Meng F; Zhong Z Emerging targeted drug delivery strategies toward ovarian cancer. Adv. Drug Deliv. Rev 2021, 178, 113969. 10.1016/j.addr.2021.113969. [PubMed: 34509574]

(19). Martin LP; Konner JA; Moore KN; Seward SM; Matulonis UA; Perez RP; Su Y; Berkenblit A; Ruiz-Soto R; Birrer MJ Characterization of folate receptor alpha (FRalpha) expression in archival tumor and biopsy samples from relapsed epithelial ovarian cancer patients: A phase I expansion study of the FRalpha-targeting antibody-drug conjugate mirvetuximab soravtansine, Gynecol. Oncol 2017, 147 (2), 402–407. 10.1016/j.ygyno.2017.03.089. [PubMed: 28843653]

(20). Cox N; Kintzing JR; Smith M; Grant GA; Cochran JR Integrin-targeting knottin peptide-drug conjugates are potent inhibitors of tumor cell proliferation, Angew Chem. Int. Ed. Engl 2016, 55 (34), 9894–9897. 10.1002/anie.201603488.

(21). Li F; Lu J; Liu J; Liang C; Wang M; Wang L; Li D; Yao H; Zhang Q; Wen J; Zhang ZK A water-soluble nucleolin aptamer-paclitaxel conjugate for tumor-specific targeting in ovarian cancer. Nat. Commun 2017, 8 (1), 1–4. 10.1038/s41467-017-01565-6. [PubMed: 28232747]

(22). Yu N; Zhang Y; Li J; Gu W; Yue S; Li B; Meng F; Sun H; Haag R; Yuan J; Zhong Z Daratumumab immunopolymersome - enabled safe and CD38 - targeted chemotherapy and depletion of multiple myeloma. Adv. Mater 2021, 33 (39), 2007787. 10.1002/adma.202007787.

(23). Baklaushev VP; Nukolova NN; Khalansky AS; Gurina OI; Yusubalieva GM; Grinenko NP; Gubskiy IL; Melnikov PA; Kardashova KS; Kabanov AV; Chekhonin VP Treatment of glioma by cisplatin-loaded nanogels conjugated with monoclonal antibodies against Cx43 and BSAT1. Drug Deliv 2015, 22 (3), 276–285. 10.3109/10717544.2013.876460. [PubMed: 24437962]

(24). Zhang Y; Yue S; Haag R; Sun H; Zhong Z An intelligent cell-selective polymersome-DM1 nanotoxin toward triple negative breast cancer. J. Control. Release 2021, 340, 331–341. 10.1016/j.jconrel.2021.11.014. [PubMed: 34774889]

(25). Soni KS; Thomas D; Caffrey T; Mehla K; Lei F; O'Connell KA; Sagar S; Lele SM; Hollingsworth MA; Radhakrishnan P; Bronich TK A polymeric nanogel-based treatment regimen for enhanced efficacy and sequential administration of synergistic drug combination in pancreatic cancer. J. Pharmaco. Exp. Ther 2019, 370 (3), 894–901. 10.1124/jpet.118.255372

(26). Cui H; Xu B Supramolecular Medicine. Chem. Soc. Rev 2017, 46 (21), 6430–6432. 10.1039/c7cs90102j. [PubMed: 29034939]

(27). Ryu JH; Chacko RT; Jiwpanich S; Bickerton S; Babu RP; Thayumanavan S Self-Cross-Linked Polymer Nanogels: A Versatile Nanoscopic Drug Delivery Platform. J. Am. Chem. Soc 2010, 132 (48), 17227–17235. 10.1021/ja1069932. [PubMed: 21077674]

(28). Zhang K; Hao L; Hurst SJ; Mirkin CA Antibody-Linked Spherical Nucleic Acids for Cellular Targeting. J. Am. Chem. Soc 2012, 134 (40), 16488–16491. 10.1021/ja306854d. [PubMed: 23020598]

(29). Upadhyay KK; Bhatt AN; Mishra AK; Dwarakanath BS; Jain S; Schatz C; Le Meins JF; Farooque A; Chandraiah G; Jain AK; Misra A; Lecommandoux S The Intracellular Drug Delivery and Anti Tumor Activity of Doxorubicin Loaded Poly(γ-Benzyl l-Glutamate)-b-Hyaluronan Polymersomes. Biomaterials 2010, 31 (10), 2882–2892. 10.1016/j.biomaterials.2009.12.043. [PubMed: 20053435]

(30). Gao J; Wu P; Fernandez A; Zhuang J; Thayumanavan S Cellular AND Gates: Synergistic Recognition to Boost Selective Uptake of Polymeric Nanoassemblies. Angew. Chemie - Int. Ed 2020, 59 (26), 10456–10460. 10.1002/anie.202002748.

(31). Gao J; Dutta K; Zhuang J; Thayumanavan S Cellular- and Subcellular-Targeted Delivery Using a Simple All-in-One Polymeric Nanoassembly. Angew. Chemie Int. Ed 2020, 59 (52), 23466–23470. 10.1002/ANIE.202008272.

(32). Wu P; Gao J; Prasad P; Dutta K; Kanjilal P; Thayumanavan S Influence of Polymer Structure and Architecture on Drug Loading and Redox-Triggered Release. Biomacromolecules 2022, 23 (1), 339–348. 10.1021/acs.biomac.1c01295. [PubMed: 34890192]

(33). Agrohia DK; Wu P; Huynh U; Thayumanavan S; Vachet RW Multiplexed Analysis of the Cellular Uptake of Polymeric Nanocarriers. Anal. Chem 2022, 94 (22), 7901–7908 10.1021/acs.analchem.2c00648. [PubMed: 35612963]

(34). Singh K; Canakci M; Kanjilal P; Williams N; Shanthalingam S; Osborne BA; Thayumanavan S Evaluation of Cellular Targeting by Fab′ vs Full-Length Antibodies in Antibody-Nanoparticle Conjugates (ANCs) Using CD4 T-Cells. Bioconjug. Chem 2022, 33 (3), 486–495. 10.1021/acs.bioconjchem.2c00024. [PubMed: 35139308]

(35). Liu B; Singh K; Gong S; Canakci M; Osborne BA; Thayumanavan S Protein–Antibody Conjugates (PACs): A Plug-and-Play Strategy for Covalent Conjugation and Targeted Intracellular Delivery of Pristine Proteins. Angew. Chemie. Int. Ed 2021, 60 (23), 12813–12818. 10.1002/ange.202103106.

(36). Goyon A; Excoffier M; Janin-Bussat MC; Bobaly B; Fekete S; Guillarme D; Beck A Determination of Isoelectric Points and Relative Charge Variants of 23 Therapeutic Monoclonal Antibodies. J. Chromatogr. B Anal. Technol. Biomed. Life Sci 2017, 1065–1066, 119–128. 10.1016/j.jchromb.2017.09.033.

(37). Johnston MC; Scott CJ Antibody Conjugated Nanoparticles as a Novel Form of Antibody Drug Conjugate Chemotherapy. Drug Discov. Today Technol 2018, 30, 63–69. 10.1016/j.ddtec.2018.10.003. [PubMed: 30553522]

(38). Marcinkowska M; Sobierajska E; Stanczyk M; Janaszewska A; Chworos A; Klajnert-Maculewicz B Conjugate of PAMAM Dendrimer, Doxorubicin and Monoclonal Antibody-Trastuzumab: The New Approach of a Well-Known Strategy. Polymers (Basel) 2018, 10 (2), 187. 10.3390/polym10020187. [PubMed: 30966223]

(39). Zacharias N; Podust VN; Kajihara KK; Leipold D; Del Rosario G; Thayer D; Dong E; Paluch M; Fischer D; Zheng K; Lei C; He J; Ng C; Su D; Liu L; Masih S; Sawyer W; Tinianow J; Marik J; Yip V; Li G; Chuh J; Morisaki JH; Park S; Zheng B; Hernandez-Barry H; Loyet KM; Xu M; Kozak KR; Phillips GL; Shen BQ; Wu C; Xu K; Yu SF; Kamath A; Rowntree RK; Reilly D; Pillow T; Polson A; Schellenberger V; Hazenbos WLW; Sadowsky J A Homogeneous High-DAR Antibody-Drug Conjugate Platform Combining THIOMAB Antibodies and XTEN Polypeptides†. Chem. Sci 2022, 13 (11), 3147–3160. 10.1039/d1sc05243h. [PubMed: 35414872]

(40). Yurkovetskiy AV; Yin M; Bodyak N; Stevenson CA; Thomas JD; Hammond CE; Qin LL; Zhu B; Gumerov DR; Ter-Ovanesyan E; Uttard A; Lowinger TB A Polymer-Based Antibody-Vinca Drug Conjugate Platform: Characterization and Preclinical Efficacy. Cancer Res 2015, 75 (16), 3365–3372. 10.1158/0008-5472.CAN-15-0129. [PubMed: 26113086]

(41). Jung JG; Kim M-S; Jung H-C; Choi H; Moon K-D Abstract 6530: Old Target, but New Approach: Targeting Cancer-Associated MUC1 with ADC and Car-T. Cancer Res 2020, 80 (16_Supplement), 6530–6530. 10.1158/1538-7445.am2020-6530.

(42). Nakai K; Hung MC; Yamaguchi H A Perspective on Anti-EGFR Therapies Targeting Triple-Negative Breast Cancer. Am. J. Cancer Res 2016, 6 (8), 1609–1623. [PubMed: 27648353]

(43). Curry JM; Thompson KJ; Rao SG; Besmer DM; Murphy AM; Grdzelishvili VZ; Ahrens WA; McKillop IH; Sindram D; Iannitti DA; Martinie JB; Mukherjee P The Use of a Novel MUC1 Antibody to Identify Cancer Stem Cells and Circulating MUC1 in Mice and Patients with Pancreatic Cancer. J. Surg. Oncol 2013, 107 (7), 713–722. 10.1002/jso.23316. [PubMed: 23335066]

(44). Zhou R; Yazdanifar M; Das Roy L; Whilding LM; Gavrill A; Maher J; Mukherjee P CAR T Cells Targeting the Tumor MUC1 Glycoprotein Reduce Triple-Negative Breast Cancer Growth. Front. Immunol 2019, 10, 1149. 10.3389/fimmu.2019.01149. [PubMed: 31178870]

(45). Moore LJ; Das Roy L; Zhou R; Grover P; Wu ST; Curry JM; Dillon LM; Puri PM; Yazdanifar M; Puri R; Mukherjee P; Dréau D Antibody-Guided in Vivo Imaging for Early Detection of Mammary Gland Tumors. Transl. Oncol 2016, 9 (4), 295–305. 10.1016/j.tranon.2016.05.001. [PubMed: 27567952]

(46). Pan D; Tang Y; Tong J; Xie C; Chen J; Feng C; Hwu P; Huang W; Zhou D An Antibody-Drug Conjugate Targeting a GSTA Glycosite-Signature Epitope of MUC1 Expressed by Non-Small Cell Lung Cancer. Cancer Med 2020, 9 (24), 9529–9540. 10.1002/cam4.3554. [PubMed: 33084221]

(47). Masuda H; Zhang D; Bartholomeusz C; Doihara H; Hortobagyi GN; Ueno NT Role of Epidermal Growth Factor Receptor in Breast Cancer. Breast Cancer Res. Treat 2012, 136 (2), 331–345. 10.1007/s10549-012-2289-9. [PubMed: 23073759]

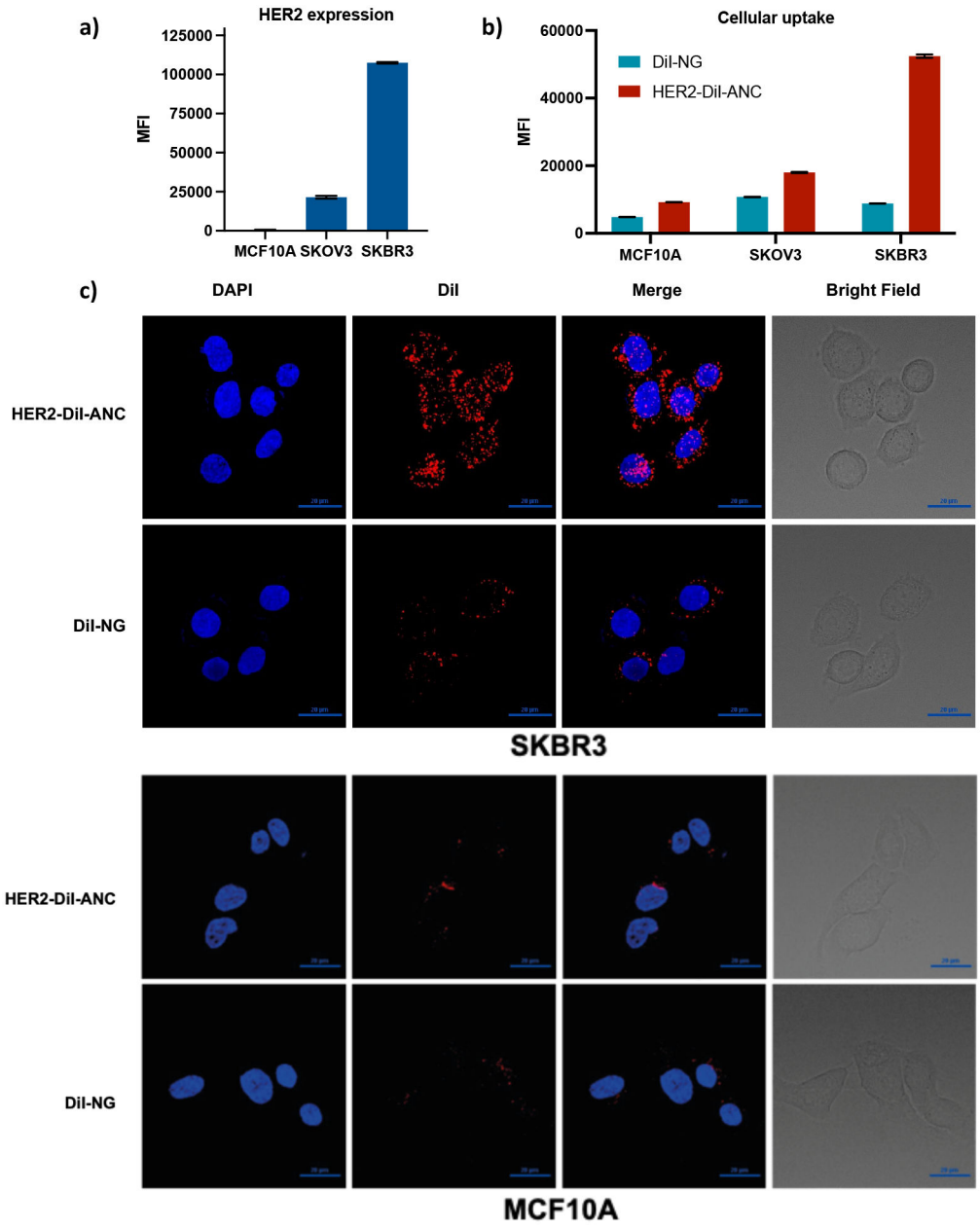

Figure 1.

HER2 expression and uptake specificity of antiHER2-ANC. a) Relative expression of HER2 in MCF10A, SKOV3 and SKBR3 measured by flow cytometry. b) Uptake of DiI encapsulated nanogels with and without antiHER2 conjugation (DiI-NG and AntiHer2-DiI-ANC, respectively) in MCF10A (HER2−), SKOV3 (HER2+) and SKBR3 (HER2+++) cells with 10 mins incubation. c) Cellular uptake of antiHER2-DiI-ANC and DiI-NG in SKBR3 and MCF10A cells analyzed by confocal imaging at 30 mins incubation.

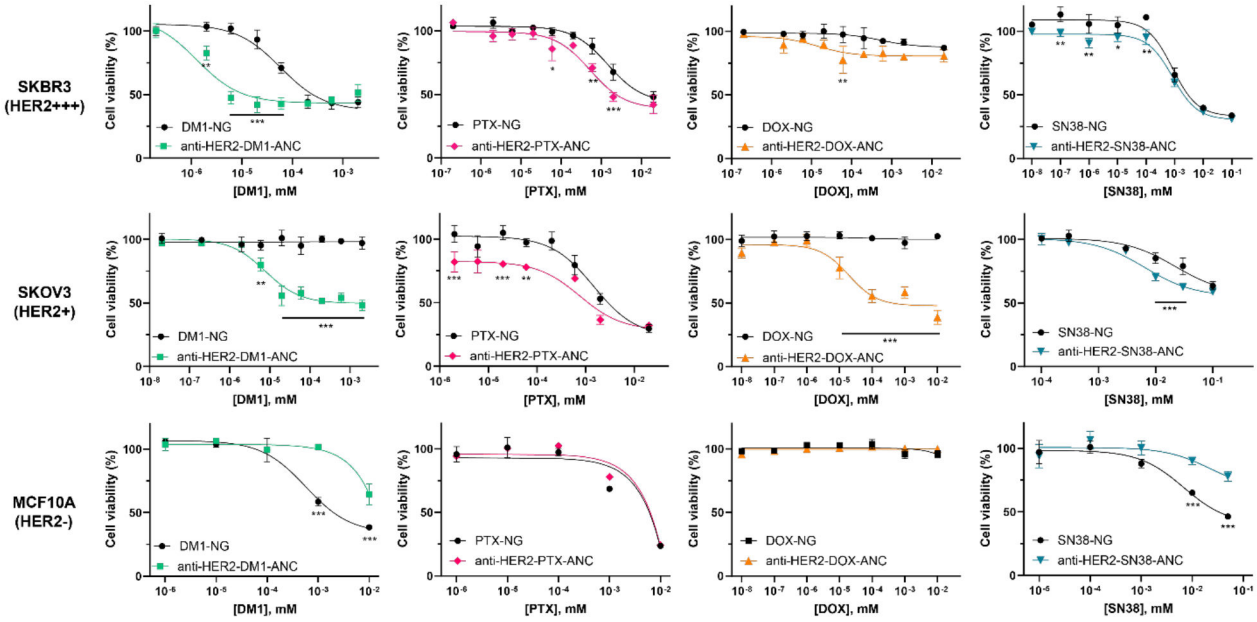

Figure 2.

Cytotoxicity of ANCs in comparison to NGs towards HER2+ (SKOV3 and SKBR3) and HER2- (MCF10A) cell lines with 10 mins incubation. Data represents means ± SD from three independent experiments. t-test analysis; *p < 0.05, **p < 0.01, ***p < 0.001.

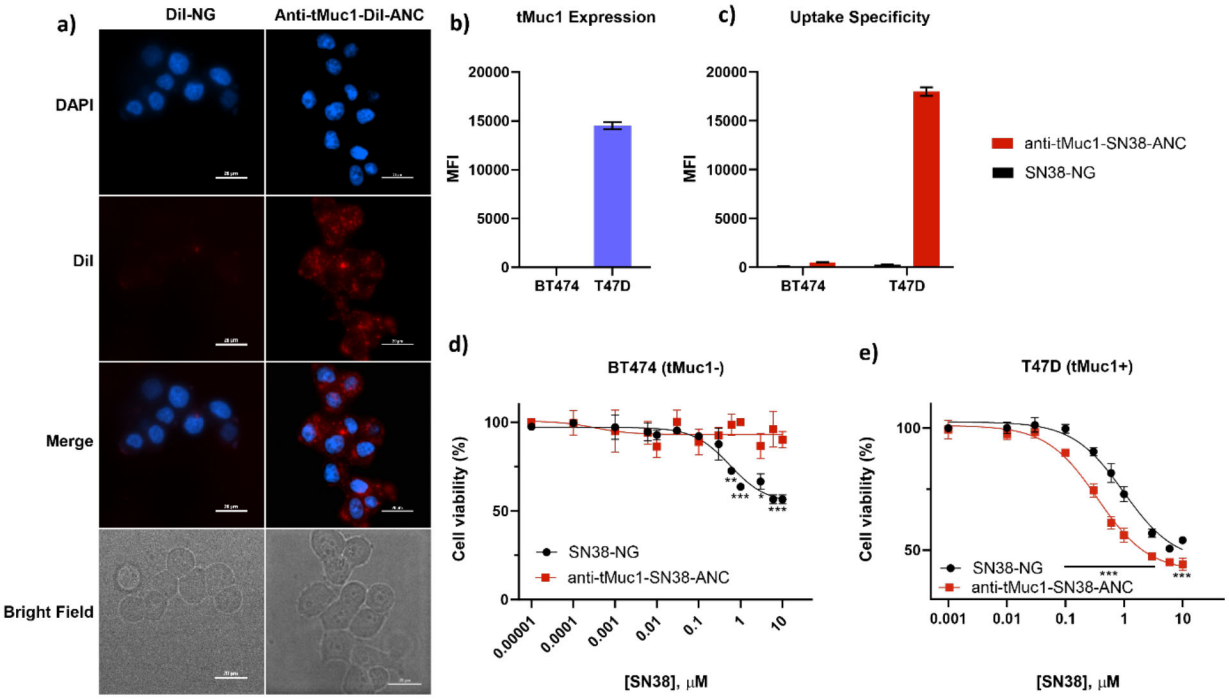

Figure 3.

Uptake specificity and cytotoxicity of tMuc1-ANCs in vitro. a) Cellular uptake of tMuc1-DiI-ANC and DiI-NG in T47D (tMuc1+) cells by confocal imaging. b) Relative expression of tMuc1 receptors in BT474 (tMuc1-) and T47D (tMuc1+) cells measured by flow cytometry. c) cellular uptake of tMuc1-DiI-ANC and DiI-NG in BT474 and T47D cells analyzed by flow cytometry. d) cytotoxicity of tMuc1-SN38-ANC in comparison to SN38-NG in BT474 and T47D cells. Data represents means ± SD from three independent experiments. t-test analysis; *p < 0.05, **p < 0.01, ***p < 0.001.

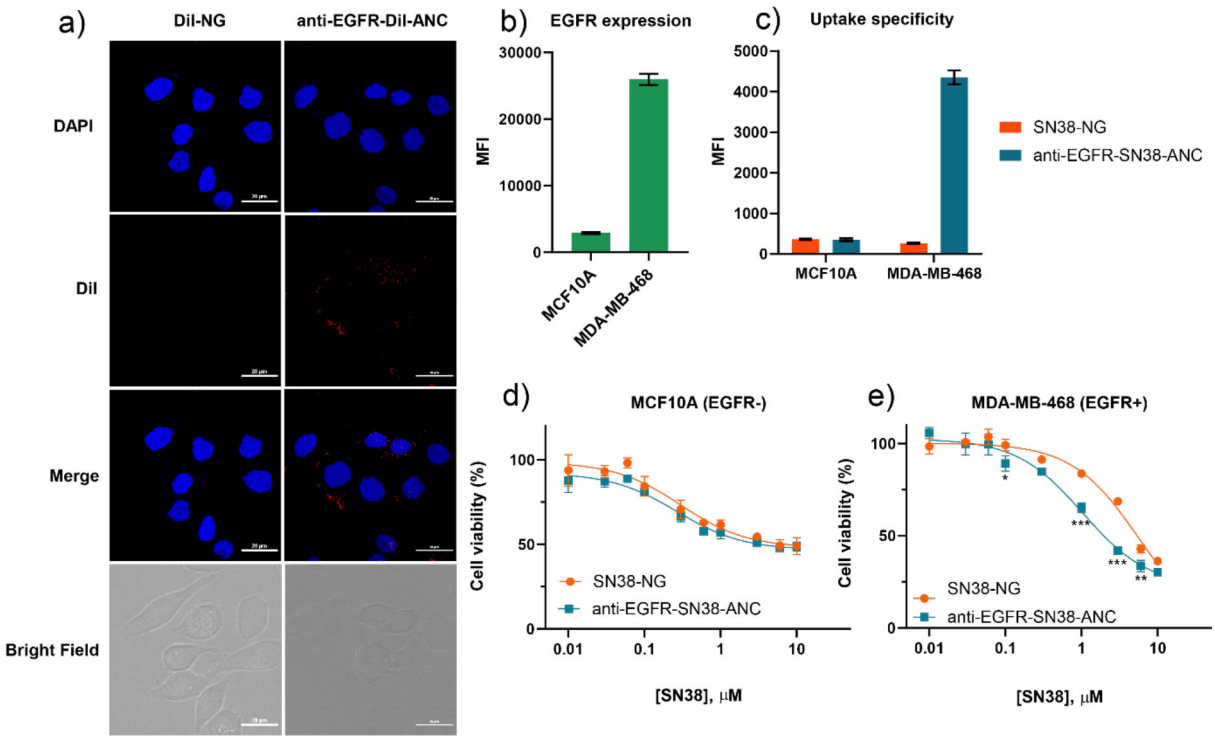

Figure 4.

Uptake specificity and cytotoxicity of EGFR-ANCs in vitro. a) Cellular uptake of EGFR-DiI-ANC and DiI-NG in TMDA-MB-468 (EGFR+) cells by confocal imaging after 10 mins incubation. b) Relative expression of EGFR receptors in MCF10A (EGFR-) and MDA-MD-468 (tMuc1+) cells measured by flow cytometry. c) cellular uptake of tMuc1-DiI-ANC and DiI-NG in MCF10A and MDA-MD-468 cells analyzed by flow cytometry. d) and e) cytotoxicity of EGFR-SN38-ANC in comparison to SN38-NG in MCF10A and MDA-MD-468 cells. Data represents means ± SD from three independent experiments. t-test analysis; *$p < 0.05$, **$p < 0.01$, ***$p < 0.001$.

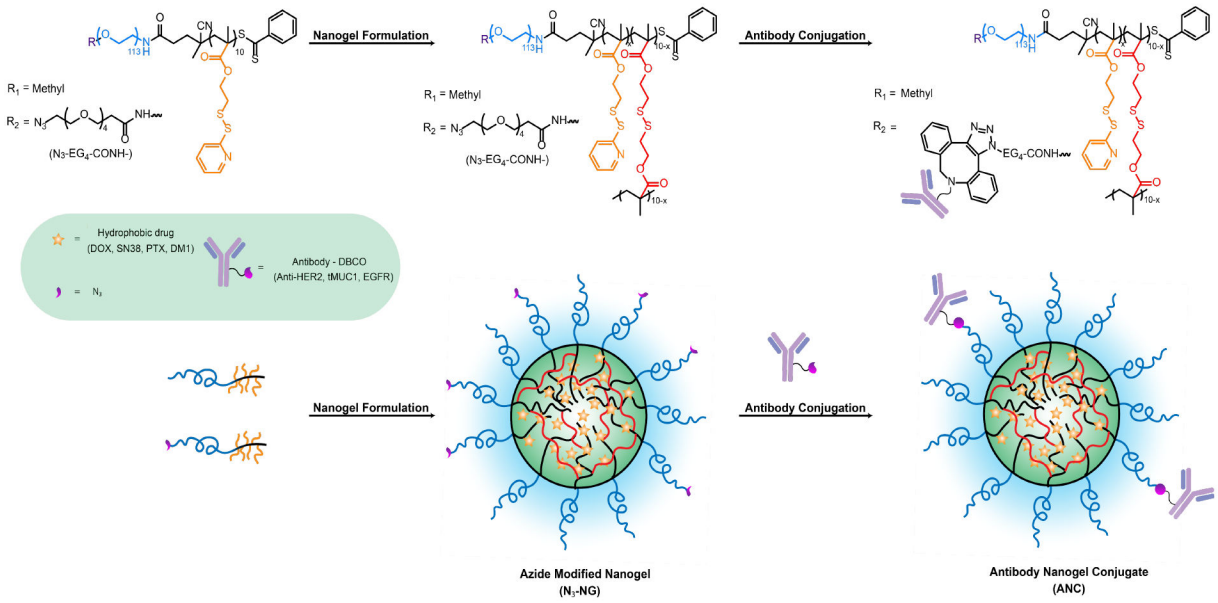

Scheme 1.

Construction of antibody nanogel conjugates (ANC) using amphiphilic block copolymer. The cargos are encapsulated in the hydrophobic pocket of the nanogel. The terminal N_3-moiety was utilized as the click handle for conjugating DBCO-modified antibody.

Table 1.

Drug to antibody ratio (DAR), encapsulation efficiency (EE) and encapsulation capacity of antiHER2 conjugated nanogels encapsulating different types of drugs.

Drug encapsulated antiHER2-ANC	DAR	EE (%)	EC (%)
PTX	2374	48	7
DOX	152	21	3
DM1	5581	24	4
SN38	2832	60	9

Table 2.

EC50 of NG and ANCs in HER2 expressing cell lines.

Vehicle	EC50 values (μM)			95% CI (range, μM)		
	SKBR3	SKOV3	MCF10A	SKBR3	SKOV3	MCF10A
DM1-NG	0.058	N.A.	0.576	0.038–0.089	N.A.	0.370–0.009
antiHER2-DM1-ANC	0.001	0.008	N.A.	0.001–0.002	0.005–0.012	N.A.
PTX-NG	1.460	1.468	N.A.	1.003–2.109	0.898–2.467	N.A.
antiHER2-PTX-ANC	0.528	0.761	N.A.	0.296–0.899	0.321–1.575	N.A.
DOX-NG	0.524	N.A.	N.A.	0.065–4.908	N.A.	N.A.
antiHER2-DOX-ANC	0.014	0.019	N.A.	0.002–0.085	0.010–0.042	N.A.
SN38-NG	0.835	22.140	6.804	0.574–1.205	9.227–61.250	0.003–0.015
antiHER2-SN38-ANC	0.844	6.473	22.050	0.602–1.176	4.178–9.876	N.A.